K-shell Auger-electron production cross sections from ion bombardment*

C. W. Woods,† Robert L. Kauffman,‡ K. A. Jamison, N. Stolterfoht,§ and Patrick Richard
Department of Physics, Kansas State University, Manhattan, Kansas 66506
(Received 19 November 1975)

We have measured the Ne K-shell electron spectra from a Ne gas target bombarded by 0.5–10 MeV H^+ and 14–21 MeV N, 24–35 MeV O, 3–35 MeV F, and 40 and 50 MeV Cl in various incident ionic charge states. The F K-shell Auger-electron spectra have been measured for F-ion collisions with Ne gas from 3 to 15 MeV. Auger-electron production cross sections are deduced. H^+ induced Ne K-shell Auger-electron production cross sections are compared to various theoretical Coulomb ionization predictions. The heavy-ion-induced Ne K-shell Auger-electron production cross sections increase with increasing projectile charge state at constant projectile energy. The F and Ne K-shell Auger-electron production cross sections from 3 to 15 MeV are favorably compared to calculations based on the molecular-orbital model.

I. INTRODUCTION

In the past few years, the production of Ne K-shell x rays[1-5] and Auger electrons[2,6-9] by both H^+ and heavy ions in the MeV energy region impinging on gas targets of Ne has been studied. The Ne K-shell x-ray production cross section increases for an increase in the ionic charge state for Cl bombardment.[2,3] High-resolution K x-ray spectra[4,5] of Ne indicate that the degree of L-shell ionization for single K-shell plus multiple L-shell ionization increases with increasing projectile charge. It is well known[10,11] that the K-shell fluorescence yield also increases as multiple L-shell ionization increases. Since the single K-shell vacancy fluorescence yield for Ne is quite small, 1.6%,[7,10] it is unclear how much of the increase in the x-ray yield is due to an increase in the fluorescence yield as opposed to an increase in the vacancy production. As previously pointed out,[2] the increase is too large to be wholly due to an increase in fluorescence yield. The object of this study is to more closely examine the projectile charge state and energy dependence of Ne K-shell vacancy production through the measurement of Auger-electron production cross sections.

The Ne x-ray measurements are further hampered by problems of absorption. For semiconductor detectors, a window, usually of Be, is necessary to separate the detector from the gas cell. For a crystal spectrometer the detector is usually a gas-flow proportional counter with a window of organic material which has a conducting (Al) film. In both cases the absorption of photons of energies of less than or approximately equal to 1 keV is severe as well as energy dependent. Relative absorption corrections needed to analyze the spectra in the crystal-spectrometer case are straightforward. In the solid-state detector case where there are many unresolved lines and the absorption varies strongly over an energy region comparable to the resolution, deconvolution is necessary. The detection of energetic electrons in approximately the same energy region by an electron multiplier is more efficient as well as much less energy dependent.

In this study a cylindrical mirror analyzer[12] was used to energy-analyze the electrons which were then detected by a continuous-channel electron multiplier. Cross sections can be deduced by comparing the number of electrons detected per the number of ions impinging on the gas cell to previously measured Ne K-shell Auger-electron production cross sections from H^+ bombardment. All cross sections are quoted relative to the determination of the 1-MeV H^+ cross section of Toburen.[13]

Included in this study is the Ne K-shell Auger-electron production cross section from H^+ impact from 0.5 to 10 MeV. This was done in order to check the operation of the analyzer where Ne K-shell Auger-electron production cross sections have been previously measured as well as to further test the Coulomb ionization theories at higher H^+ energy where the assumptions made in these theories should be more accurate. The cross section for Cl bombardment is presented and compared to previous measurements. The nuclear-charge- and atomic-charge-state dependence of the Auger-electron production cross section for fixed projectile velocity is investigated for H, N, O, and F projectiles. The energy dependence of the F projectile case is presented for bombarding energies of 3–35 MeV. F projectile and Ne target cross sections are presented and compared to calculations based on the molecular-orbital (MO) model in this intermediate-energy region.

II. EXPERIMENTAL ARRANGEMENT

The experiment consisted of measuring the yield of electrons from collisions of ions with Ne

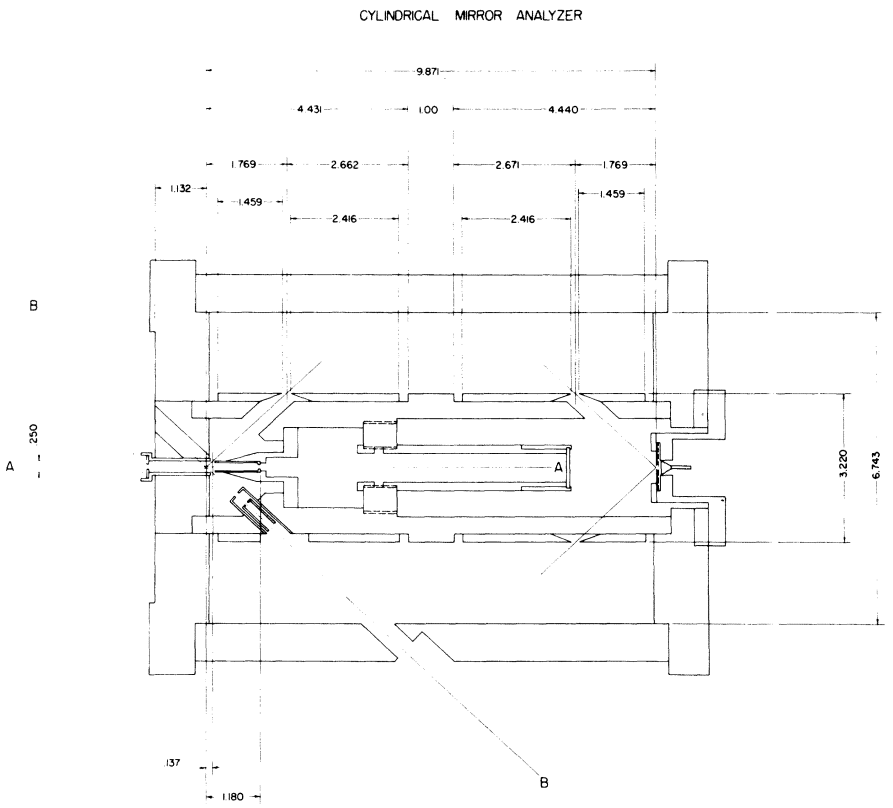

FIG. 1. Scale drawing of the cylindrical mirror analyzer with measured dimensions (in meters). The line labeled A is the beam axis for the forward mode. The line labeled B is the beam axis for the backward mode.

gas as a function of electron energy. The electron energy was determined with a cylindrical mirror analyzer and the electrons detected with a continuous-channel electron multiplier (channeltron). At the same time the beam current was integrated to measure the number of incident ions. For experiments performed at the tandem Van de Graaff accelerator a PDP-15 computer was used to record the electron energy distribution and for measurements at the 3-MV Van de Graaff a Nuclear Data ND100 1024-channel analyzer was used. In both cases the PDP-15 computer was used to analyze the data.

The cylindrical mirror analyzer was designed and constructed at KSU.[14] Figure 1 is a scale drawing, with measured dimensions of the completed analyzer. The inner and outer cylinders have diameters of about $3\frac{1}{2}$ and $6\frac{3}{4}$ in. (8.8 and 17 cm) respectively, whereas the image and object positions are separated by $9\frac{3}{4}$ in. (25 cm). Two concentric cylinders of magnetic shield material with diameters of 9 and 10 in. (23 and 25 cm) and length of 20 in. (51 cm) were placed around the analyzer to reduce the Earth's magnetic field. It has the unique feature of being able to have the axis of the analyzer aligned either with the ion-beam direction or rotated to an angle of 132° to the ion-beam direction. In the aligned, or forward, position electrons emitted at 42° in the laboratory frame are analyzed. In the rotated, or backward, position electrons ejected at angles from 90° to 174° are analyzed. All measurements with heavy-ion projectiles were made with the analyzer in the backward position except those measurements which included beam Auger spectra. This was done to reduce the background associated with both collisionally produced electrons which are mainly forward peaked[10] and beam Auger electrons which are kinematically forward peaked. The H^+ induced spectra were measured in both positions.

The resolution of the analyzer (peak base width) depends on the widths of the entrance and exit slits and the size of the ion beam. An approximate theoretical base width given by Risley[12] was used to estimate the energy resolution of our analyzer for the case of equal entrance and exit slits. The results are given in Table I. The measured resolution using the Ne ^1P diagram line at 772 eV is 1.4% for 2-mm beam diameter and 1.0-mm entrance and exit slit widths. The discrepancy between the calculated and measured resolution is not large considering the difficulty in determining the background due to the other Auger peaks. The difference could be due to the inaccuracies in the background estimate, kinematic

TABLE I. Calculated base width of KSU cylindrical mirror analyzer in % and eV for 800-eV electrons.

Beam diameter	Resolution % and energy [a] $\chi = 0.25$ mm %	ΔE(eV)	$\chi = 0.50$ mm %	ΔE(eV)	$\chi = 1.0$ mm %	ΔE(eV)
1 mm	0.26	2.1	0.47	3.8	0.88	7.1
2 mm	0.44	3.5	0.65	5.2	1.06	8.5

[a] χ is the entrance and exit slit width. Three values of χ of 0.25, 0.5, and 1.0 mm are given.

broadening, or distortion due to finite voltage-sweep speed.

A Bendix channeltron was used to detect the energy-analyzed electrons. The efficiency of such a device has been measured by several authors.[15,16] Its efficiency for electrons in the energy region 600–1000 eV is approximately 90% and only slowly energy dependent. The efficiency is sensitive to extremely high count rates, gas exposure, and degradation due to total electron exposure. We only assume that this efficiency does not change over short periods of time since we renormalize by repeating H^+ bombardment of Ne every few hours.

Figure 2 is a block diagram of the electronics used in the experiment. With 2800–3000 V on the channeltron and the amplifier gain properly chosen, an electron event gives a pulse of 3–5 V while the noise level is less than 0.5 V. A single-channel analyzer was used to distinguish an electron event from the noise. The outer-cylinder voltage divided by a factor of 1000 and amplified by a factor of about 4 is fed to a linear gate which is triggered each time the channeltron registers an electron event. This pulse is then inverted and fed to an analog-to-digital converter connected either to a PDP-15 computer or a Nuclear Data ND100 multichannel analyzer. The voltage between the plates is provided by a programmable high-voltage supply. The programmable supply is controlled by a function generator which produces a triangular voltage sweep and is floated to a reference voltage. The voltage between the cylinders is thus of a triangular sweep centered about a reference voltage. The finite capacitance of the analyzer can cause distortion,[17] and care was taken to minimize this effect. A white spectrum was taken at several sweep rates and small but visible distortion of the end points of the spectrum occurred for sweep rates above 10 Hz. The data was taken with the sweep rate set at less than 2 Hz.

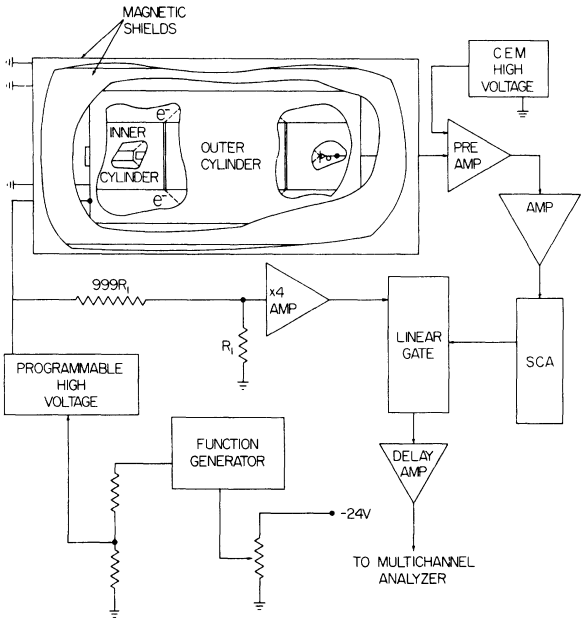

FIG. 2. Block diagram of the electronics used including the cylindrical mirror analyzer. The notation and function of the electronics are discussed in the text.

The analyzer has a designed ratio of the electron energy E to the voltage between the cylinders, V, of $R = E/V = 1.772$. This ratio was measured with a Fluke differential voltmeter, pulse-height analysis with the PDP-15 computer, and the 2-MeV H^+-induced Ne ^1D diagram line, to be $1.76 \pm 1\%$. Since the theoretical value lies within the measured ratio, the theoretical value R was used. Energy calibration was accomplished by setting the voltage between the cylinders (usually 100–1000 V in 50-V intervals) using a pulser in place of the channeltron to initiate counting. In all cases a linear fit was used to convert from channel to voltage, and then R was used to convert from channel to energy. The energy calibration is accurate to 1%.

The ion beams used in the experiment were obtained from two sources. The heavy-ion beams and H^+ beams of 1–10 MeV were produced by the EN tandem Van de Graaff at the Nuclear Sciences Laboratory at Kansas State University. H^+ beams of 0.5–2 MeV were produced by the AK Van de Graaff at Kansas State University. The various charge states of the heavy ions were produced by accelerating and magnetically analyzing the desired charge states were practical. In other cases the desired charge states were produced by accelerating the primary charge state which produced the largest beam intensity at the desired energy and then passing this beam through a thin (10–20 $\mu g/cm^2$) carbon foil. The beam comes to a charge-state equilibrium in the foil with a very small loss in energy. The resulting charge states were mag-

netically analyzed by a second magnet and sent through the gas cell. A quadrupole lens was used to focus the beam through the gas cell. The Ne gas pressure in the gas cell was monitored by a thermocouple gauge and maintained by either a mechanical leak valve or a manually controlled automatic pressure controller. This pressure was usually set at 10–20 mTorr. It is important that the absolute pressure not be too large so that the mean charge state of the beam remains approximately the incident charge state. The pressure need not be accurately known because H^+ bombardment of Ne is used to normalize the cross-section determination. Tests were made with F^{+3} at 3 and 5 MeV, where the charge-transfer cross sections should be large, to investigate the yield as a function of pressure. In all cases the yield and the pressure reading varied linearly with the H^+ normalization from 5 to 20 mTorr as read on the thermocouple gauge. Tests of the mean charge state were also run with these beams by measuring the beam current registered in the Faraday cup with gas in the cell and gas out of the cell. No change in the current registered by the current integrator could be detected. This is not an accurate determination of the mean charge state, but does add confidence that large charge changing effects (>10%) are not occurring.

Typical runs consisted of setting the gas pressure, calibrating the multichannel analyzer, running a normalization run with 2- or 1-MeV H^+ and then running H^+, N^{+q}, O^{+q}, or F^{+q}. As soon as a run was completed, typically 1 h for the heavy ions and $\frac{1}{2}$ h for the H^+, the pressure in the gas cell was checked again. After several runs, or if a pressure variation was noted, an H^+ normalization was run again. Over a typical running period, one to two days, the H^+ normalization repeated within ± 5% when care was taken to insure no change in Ne pressure.

III. DATA ANALYSIS

The analysis of the data was accomplished with a PDP-15 computer in the Nuclear Science Laboratory of Kansas State University. A single computer program was developed to display the electron spectra, fit the collisionally produced electron background in the vicinity of the Auger-electron peaks, and extract the Auger-electron yield. The program then calculated the cross section using the Auger yield and the normalization parameters.

The electron background was fit with a polynomial least-squares technique.[18] To facilitate fitting the rapidly decreasing background for the H^+ bombardment observed in the forward position and all the heavy-ion bombardment data the log of the data was fit to a polynomial. The functional form assumed for the background was, thus, either a polynomial of degree less than or equal to 3 or an exponential of a polynomial of degree less than or equal to 3. This fit was accomplished by simultaneously fitting approximately 25 data points at higher energy and 25 data points at lower energy than the Auger-electron peaks. The fit to the background was then superimposed over the spectra on the oscilloscope connected to the computer. In general, the simplest function which gave reasonable extrapolation of the background, as determined by the person reducing the data, was used.

Since the natural linewidths (neglecting kinematic broadening) are much smaller than the instrument resolution, a dispersion correction was made. The dispersion $\Delta E/E$ of the analyzer is constant so this correction involves dividing the measured intensity by the electron energy.

The cross section σ is then given by

$$\sigma = C\left(\frac{q}{Q}\right)\sum_i \frac{I(i)-B(i)}{E(i)}\,, \tag{1}$$

where q is the incident-ion atomic charge state, Q is the integrated charge collected in the Faraday cup, i is the data channel, $I(i)$ is the measured intensity in channel i, $B(i)$ is the background in channel i, $E(i)$ is the electron energy for channel i, and C is a normalization constant. We have made the assumptions that the ions do not change charge state in the apparatus and that the emission of Auger electrons is isotropic. For Auger electrons emitted by the beam an additional correction is necessary to account for the kinematics and this correction will be discussed when the data are presented. The normalization constant C was evaluated using the Auger-electron yield from either 1- or 2-MeV H^+-bombarded Ne using either $\sigma = 0.85 \times 10^{-19}$ cm^2 for 1-MeV H^+ or $\sigma = 1.0 \times 10^{-19}$ cm^2 for 2-MeV H^+.[19] Previously published preliminary results were normalized to 1.18×10^{-19} cm^2 for 2-MeV H^+ bombardment and should be lowered by 15%.[20,21] The value of C varied because of changes in channeltron efficiency, changes in target gas pressure, changes in the voltage sweep range, and changes in the analyzer configuration (slit widths, etc.) and was considered constant only between proton normalization runs.

It is important to estimate the possible errors inherent in the determination of the cross sections by Eq. (1). The random errors due to counting statistics are small (<3%), since there were hundreds to thousands of counts in each channel and the sum extends over many channels, but the possible systematic uncertainties are large. The

uncertainty given by Toburen for the 1-MeV H^+ cross section is 10%.[13] The principal systematic errors can arise from the analyzer transmission and detector efficiency, kinematic effects, target pressure variations, beam-current integration, the assumption of charge-state purity, and uncertainties in the data analysis.

Assuming the errors are independent, we estimate the overall relative uncertainties for H^+ bombardment are about 10% and for heavy-ion bombardment are about 15%. The energy dependence of the cross sections is uncertain to 10%. At fixed energy the charge-state dependences of the heavy-ion results is uncertain to 15%. We estimate that the absolute values are accurate to 20% for the H^+ bombardment and 25% for the heavy-ion bombardment.

IV. RESULTS

The spectra from H^+ impact and heavy-ion impact are quite different and perturbation theories involving the Coulomb interaction are expected to give better results for H^+ bombardment. We choose to present the results separately for H^+ bombardment and heavy-ion bombardment.

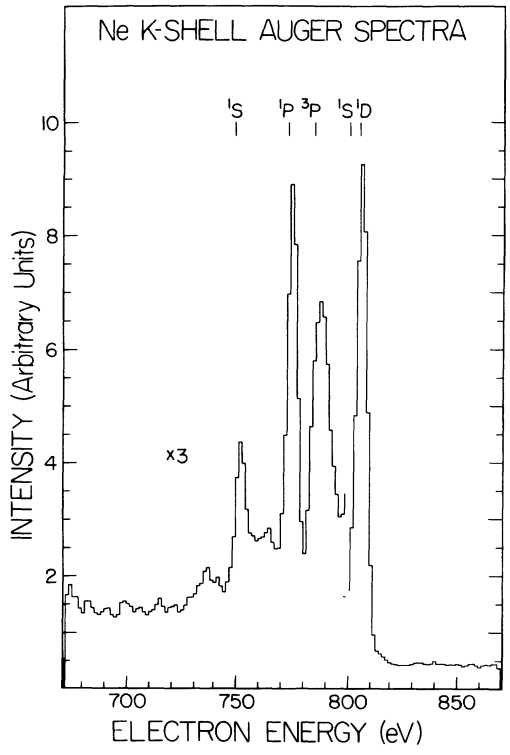

FIG. 3. Ne K-shell Auger-electron spectrum for 1.5-MeV H^+ bombardment. The diagram line positions are indicated. The electron peak corresponding to the ^3P diagram line contains intensity from multiple L-shell vacancy states as well as the diagram line. The ^1S diagram line is not resolved from the ^1D diagram line with the analyzer used. The ^1S intensity is expected to be 20% of the ^1D intensity.

A. H^+ bombardment

Figure 3 shows the electron energy spectrum observed with 1.5-MeV H^+ bombardment. The spectrum is essentially the same as that given by Schneider *et al.*[7] The spectral features are similar to those given by Edwards and Rudd[22] for 300-keV H^+ bombardment and Matthews *et al.*[5] for 0.25- and 6.0-MeV H^+ bombardment, both of which have much better resolution. Krause *et al.*[23,24] have identified many of the lines from high-resolution measurements of Ne K-shell Auger electrons following electron and photon bombardment. The H^+-induced Ne K-shell Auger-electron spectra are dominated by the diagram lines due to single K-shell vacancies indicated in the upper part of Fig. 3. The K-$L_{2,3}L_{2,3}$ transition to a ^1S final state (here the final state refers to the two holes in the ion after Auger-electron emission) is not resolved from the same transition to a ^1D final state by our analyzer. The ^1S final state is expected to be weaker by a factor of about 5.[5,22–24] The peak corresponding to the energy of the K-$L_1L_{2,3}$ transition to the ^3P final state contains intensity from many closely spaced lines from $KL_{2,3}$-$L^3_{2,3}$ type transitions as well as the diagram line. Many more lines are resolved with better resolution[5,22–24] and they appear as a continuum with the resolution of

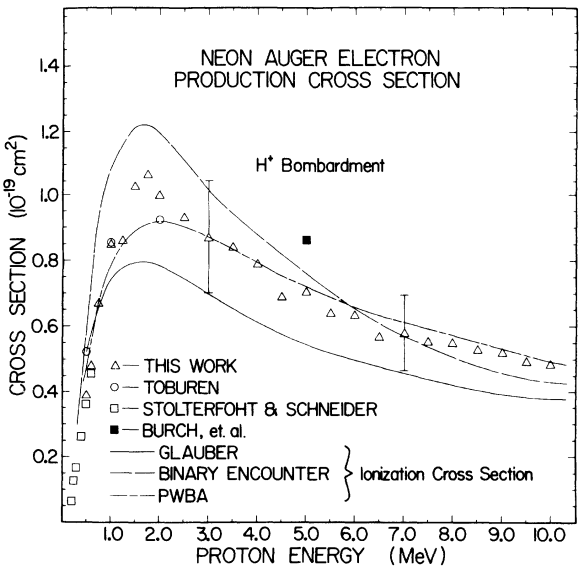

FIG. 4. Ne K-shell Auger-electron production cross sections for H^+ bombardment as a function of H^+ energy. Previously reported cross sections are given as well as theoretical predictions for the ionization cross section.

TABLE II. Ne K-shell auger cross sections from H^+ bombardment.

H^+ energy (MeV)	Cross section [a] (10^{-20} cm^2)	H^+ energy (MeV)	Cross section [a] (10^{-20} cm^2)
0.15	0.28 [b]	3.5	8.4
0.20	0.62 [b]	4.0	7.9
0.25	1.25 [b]	4.5	6.9
0.30	1.66 [b]	5.0	7.0, 8.6 [d]
0.40	2.6 [b]	5.5	6.4
0.50	3.9, 3.5 [b], 5.2 [c]	6.0	6.4
0.60	4.8, 4.5 [c]	6.5	5.7
0.75	6.7	7.0	5.8
1.00	(0.85), 0.85 [c]	7.5	5.5
1.25	8.6	8.0	5.5
1.50	10.4	8.5	5.3
1.75	10.7	9.0	5.2
2.0	10.0, 9.2 [c]	9.5	5.0
2.5	9.3	10.0	4.8
3.0	8.7		

[a] The total absolute uncertainty for the present measurements is 20% and the energy-dependence uncertainty is 10%.

[b] Stolterfoht and Schneider, Ref. 25.

[c] Toburen, Ref. 13.

[d] Burch *et al.*, Ref. 3.

our analyzer.

Figure 4 shows the cross sections obtained for 0.5–10-MeV H^+ bombardment. Also shown are the data of Toburen,[13] the data of Stolterfoht and Schneider,[25] and that of Burch *et al.*[3] All the data are consistent within the experimental uncertainties. The experimental values used in Fig. 4 are given in Table II. Since the fluorescence yield is small for the states populated by H^+ bombardment and charge exchange and molecular effects are expected to be small, we can compare the Auger production cross sections directly to the Coulomb ionization predictions based on various approximations. We have plotted the predictions of the binary-encounter approximation[26] (BEA), plane-wave Born approximation[27] (PWBA), and a recent Glauber-approximation calculation[28] in Fig. 4. The simple BEA theory predicts the order of magnitude, but not the energy dependence, of the cross section from about 0.4 to 10 MeV. The PWBA calculation agrees very well with the data from 2 to 10 MeV. The most important test is whether the theories predict the energy dependence of the cross sections. The quantum-mechanical theories can be raised or lowered by about 20% by judicious choice of the wave functions or the limits of integration.[29] Indeed, the PWBA and Glauber calculations should be identical in the high-energy limit if the same wave functions and integration limits are used. The total uncertainty in the data has been discussed and is about 20%. If these theoretical predictions are normalized to the data at 10 MeV, then the Glauber calculation fits within ±5% down to about 2 MeV and the PWBA fits down to 2.5 MeV. Within the experimental uncertainty in energy dependence of 10% (half that indicated by the error bars) the Glauber and PWBA energy dependences agree with the data from 2 to 10 MeV.

B. Heavy-ion bombardment

It is most natural to present the heavy-ion results in two sections. The first is the presentation of the Ne K-shell Auger-electron spectra and cross sections for the heavy-ion projectiles. The second section will deal with the F projectile cross sections measured to compare with the predictions of the molecular-orbital model. Included in this section will be a discussion of the corrections for the kinematic effects.

1. Ne target spectra and cross sections

Figure 5 gives a comparison of the proton- and heavy-ion-induced spectra measured in the back-

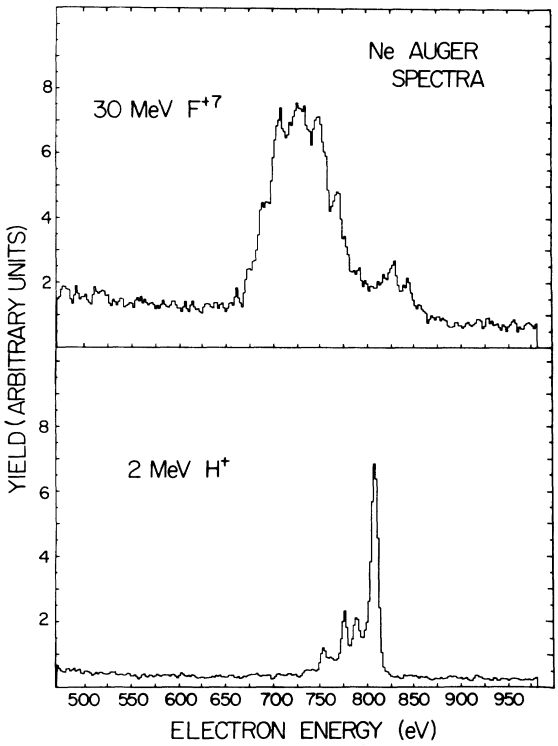

FIG. 5. Ne K-shell Auger-electron spectra for 2-MeV H^+ bombardment and 30-MeV F^{+7} bombardment. Most of the electron intensity is shifted to lower energy due to multiple L-shell ionization for heavy-ion bombardment. The intensity above 80 eV is due to K-LM type transitions. The small peak at 660 eV is due to Li-like Ne and is the lowest-energy line expected for Ne K-shell Auger electrons.

TABLE III. Ne K-shell Auger-production cross sections (10^{-19} cm^2).

Energy (MeV)	Projectile																			
	N^{+4}	N^{+5}	N^{+6}	N^{+7}	O^{+4}	O^{+5}	O^{+6}	O^{+7}	O^{+8}	F^{+3}	F^{+5}	F^{+6}	F^{+7}	F^{+8}	F^{+9}	Cl^{+7}	Cl^{+8}	Cl^{+11}	Cl^{+12}	Cl^{+13}
3										4.5										
4										6.0										
5										6.1	7.5									
7.5										8.8	8.0									
10.0										10.4	10.7		31							
12.5										14.6	11.9		28							
14	12	22	50	83																
15										14.8	18.6		32	80						
17.5										15.6	17.3									
19	14	28	51	84																
20										16.4	22		37	75	110					
21				80																
22.5											20									
24					29	28	38	70	115											
25											28		40	76	114					
27.5													40	83	97					
28.5											33	29	44	70	109					
30						34	46	67	100				43	78	110					
35							44	62	101						106					
40																31		62	60	71
50																30[a]	53, 65[a]		75[a]	100[a]

[a] Date from Burch *et al.*, Ref. 3.

ward mode. Most of the electron intensity is shifted to lower energy owing to multiple L-shell ionization for heavy-ion bombardment. The intensity above 800 eV is due to K-LM type transitions with the M-shell electron coming from excitation or capture. The small peak at 660 eV is due to Li-like Ne and is the lowest energy line expected for Ne K-shell Auger electrons.

The spectra for the various heavy-ion bombardment are quite similar. At fixed projectile energy the centroid energy of the electron distribution shifts to lower electron energy with increasing projectile charge state indicating an increase in multiple L-shell ionization[30] as projectile charge-state increases. The Ne K-shell Auger electron spectra produced by bombardment with bare nuclear projectiles of N, O, and F contain intensity from initial states with double K-shell vacancies, as previously reported.[31]

The Ne K-shell Auger production cross sections are given in Table III. Also given in Table III are the Cl-induced cross sections measured by Burch *et al.*[3] Two trends in the N-, O-, and F-induced data can be seen in Table III. When a K-shell vacancy is present in the projectile, the cross sections remain constant or decrease with increasing projectile energy. When no initial K-shell vacancies are present in the projectile, the cross sections increase with increasing projectile energy. In the energy range studied the Coulomb ionization prediction increases with increasing projectile energy,[26,27] while charge capture from the target K-shell to the projectile K-shell is decreasing with increasing projectile energy.[32] When K-electronic exchange is possible, the energy dependence of the Ne K-shell Auger-electron production cross sections reflect the importance of this process in creating Ne K-shell vacancies with N, O, and F projectiles.

As previously pointed out,[21] the energy dependence of the Ne K-shell Auger-electron production cross sections for F bombardment in incident charge states $q < 8+0$ is predicted by Coulomb ionization down to about 15 MeV. Below 15 MeV the measured cross section falls off more slowly than the Coulomb ionization prediction. We believe this is due to the fact that molecular-orbital promotion[33-35] and vacancy sharing[36] are important for producing Ne K-shell vacancies by F projectiles at incident energies below 15 MeV.

Finally, it must be pointed out that the data given in Table III indicate that Ne K-shell vacancy production increases with increasing projectile charge state at fixed projectile energy. This increase is most dramatic when K-shell electrons are removed from the projectile. This is reasonable since K-electronic exchange becomes possible and the K-shell electrons should screen the projectile nucleus more effectively than the L-shell electrons.

2. *F projectile cross sections*

When the projectile velocity is small compared to the orbital velocity of the bound electrons, it is possible to describe the collision in terms of a time-dependent quasimolecule.[32-36]

Within such a molecular-orbital model (MO), inner-shell vacancies are produced by transfer of inner-shell electrons to vacant outer-shell orbitals during the collision. The electrons are assumed to occupy molecular states appropriate to the colliding nuclei separated by a fixed distance. The relative motion of the colliding pair is assumed to provide a coupling which allows transfer of electrons to vacant orbitals. When the nuclei are well separated, they are essentially moving toward or away from one another. This gives rise to a radial coupling which allows transfer between orbitals of similar orbital angular momentum. When the colliding nuclei are close together, they are rotating about their center of mass. This rotation gives rise to a rotational coupling which allows transfer between orbitals of differing orbital angular momentum. The dominant mechanism for producing K-shell vacancies is the rotational coupling between the $2p\pi_x$ molecular orbital and the $2p\sigma$ molecular orbital at close internuclear separation. As the nuclei recede from one another, a radial coupling between the $2p\sigma$ and $1s\sigma$ molecular orbitals gives rise to transfer between these orbitals. At large internuclear separation the $1s\sigma$ orbital is correlated to the K shell of the larger-Z partner in the collision, the $2p\sigma$ orbital is correlated to the K shell of the smaller-Z partner, and the $2p\pi_x$ orbital is correlated to the $2p$ atomic orbital of the larger-Z partner. Thus, for a K-shell vacancy to be produced in the collision, a $2p\pi_x$ vacancy must be brought into the collision. For F ions on Ne this corresponds to a vacancy in the Ne $2p$ subshell before the collision. Such vacancies must be produced in the collision since Ne has no $2p$ vacancies initially. If a two-state calculation is performed by considering only the radial coupling between the $2p\pi_x$ and $2p\sigma$ molecular orbitals, the total K-shell vacancy production (F and Ne) can be calculated.[35] If only the radial coupling between the $2p\sigma$ and $1s\sigma$ orbitals is considered, a K-shell vacancy sharing ratio can be calculated.[36]

The MO model requires that the electrons have sufficient time to adjust during the collision. A sufficient condition for this to be the case is for the initial velocity of the ion to be much less than the velocity of a $2p$ electron in the united atom. This requires, for F on Ne, that the F energy be much less than 10 MeV. The energy range studied is thus at the upper regions that one might expect such a model to be applicable. It will be shown that this model gives quantitative results in agreement with the experimental data.

Meyerhof[36] has given a vacancy sharing ratio based on the work of Demkov.[37] This ratio R of the larger-Z cross section to the smaller-Z

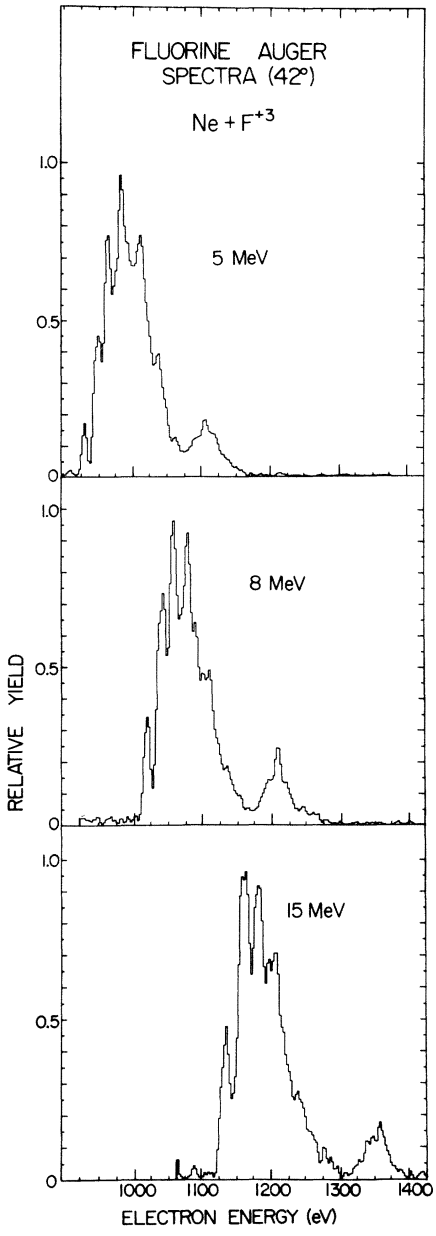

FIG. 6. F K-shell Auger-electron spectra for F^{+3} on Ne at 5-, 8-, and 15-MeV F bombarding energy. These spectra were measured with the analyzer in the forward mode. A background of the exponential form, as discussed in the data analysis section, has been subtracted from the spectra. The data have been divided by the electron energy to correct for the dispersion of the analyzer.

cross section is given by

$$R = e^{-2|x|},$$

with

$$x = \frac{\pi(I_1 - I_2)}{(2m)^{1/2}(I_1^{1/2} + I_2^{1/2})v},$$

where I_1 and I_2 are the projectile and target K-shell ionization potentials, v is the projectile velocity, and m is the electron mass. For F on Ne the value of x is

$$x = -1.40/v,$$

where v is the projectile velocity in a.u. In order to test this prediction, we have measured the F projectile cross sections in the energy region of 3–15 MeV.

Since the projectile velocities used were of the order of the ejected Auger-electron velocities, the projectile cross sections were measured with the analyzer in the forward mode (42°). The ejected electrons are shifted in energy, and the rest-frame energy E' is given in terms of the observed energy E by[30]

$$E' = E - 2(Et)^{1/2}\cos\theta\cos\beta + t,$$

where θ is the observation angle (42°), β is the angle to which the projectile is scattered, and t, the reduced energy, is given by $t = T/\lambda$ where T is the projectile energy and λ is the projectile mass in electron mass units. We make the further assumption that β is small and can be set to 0. This should be a better approximation as the energy increases and calculations based on a simplified impact-parameter model give $\beta \lesssim 0.1$ for 99% of the cross section for the lowest energy studied. Figure 6 gives the observed electron energy distributions for various energies of F^{+3} bombardment of Ne. An exponential background as discussed in the data analysis has been subtracted from the spectra.

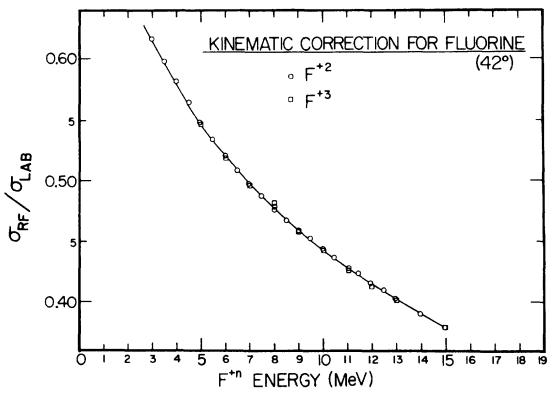

FIG. 7. Total kinematic corrections (σ_{RF}/σ_{LAB}) is displayed as a function of F energy.

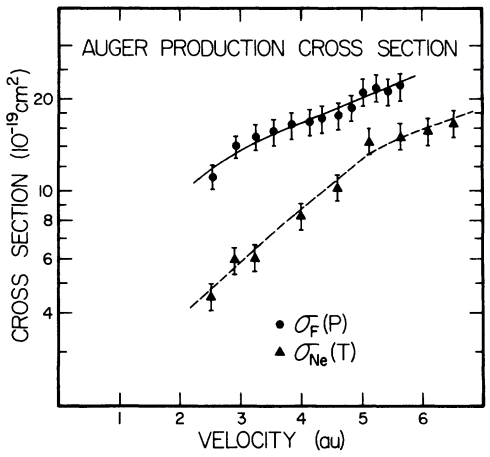

FIG. 8. F and Ne K-shell Auger-electron production cross sections from 3- to 15-MeV F projectile energy as a function of projectile velocity in a.u. The F cross sections were measured in the forward mode and are an average of the cross sections for F^{+2} and F^{+3} bombardment. The Ne cross sections were measured in the backward mode and are for F^{+3} bombardment.

The fact that the electrons are emitted from moving ions necessitates a correction to obtain the rest-frame intensity per sr, I', from the observed intensity per sr, I. If $d\Omega'$ and $d\Omega$ are the corresponding solid angles, then a simple analysis based on $I'\,d\Omega' = I\,d\Omega$ gives[30]

$$I'/I = (E'/E)[1 - (t/E')\sin^2\theta]^{1/2}.$$

Cross sections are then extracted from the spectra by using Eq. (1) with $I(i)$ replaced by $I'(i)$. Figure

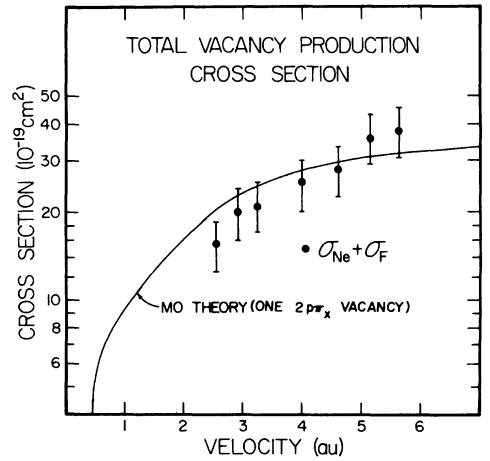

FIG. 9. Total K-shell Auger-electron production cross sections ($\sigma_{Ne}+\sigma_F$) as a function of F projectile velocity in a.u. Also given in the figure is the two-state rotational coupling calculation of Taulbjerg. The theoretical cross section is for one $2p\pi_x$ vacancy early in the collision.

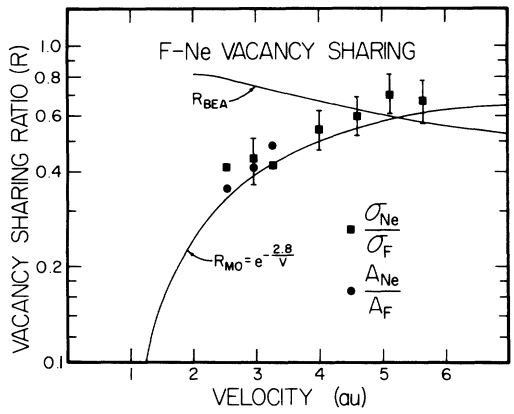

FIG. 10. Ratio of the Ne K-shell Auger-electron production cross section to the F K-shell Auger-electron production cross section as a function of F projectile velocity in a.u. Also given in the figure is the molecular-orbital prediction of Meyerhof and the prediction for Coulomb ionization from the BEA.

7 gives the overall kinematic corrections, σ_{RF}/σ_{LAB}, for various F energies, where RF and LAB refer to rest frame and lab frame, respectively.

Figure 8 gives the F-on-Ne cross sections as a function of F velocity. Since the gas cell is longer in the forward direction, it was necessary to measure the cross sections at 4 mTorr Ne pressure. The F cross sections given are an average of the F^{+2} and F^{+3} cross sections. These cross sections were found to be equal within experimental errors in the energy range studied. Since Ne is the higher-Z partner in the collision, any $2p\pi_x$ molecular vacancies which would be rotationally coupled to the F K-shell during the collision would come either from long-range interactions early in the collision[30] or from ionization near the distance of closest approach.[38] We expect that the velocity-dependent component of the $2p\pi_x$ vacancy probability[30] should dominate and the K-shell vacancy production should not change appreciably from F^{+2} to F^{+3}. The Ne cross sections given in Fig. 10 were measured in the backward mode.

Figure 9 compares the total vacancy production (F + Ne cross section) to the prediction of a two-state rotational coupling model calculated by Taulbjerg.[39] The theoretical curve is for one initial vacancy in the $2p\pi_x$ molecular orbital, and we have assumed that the correction for Auger yield can be ignored. One vacancy in the $2p\pi_x$ molecular orbital corresponds to three vacancies in the Ne $2p$ level early in the collision.

Figure 10 gives the cross-section ratio ($R = \sigma_{Ne}/\sigma_F$) as a function of F projectile velocity. The Ne cross sections were measured in the backward mode. At low F energy (3–5 MeV) it was possible to extract the Ne and F areas from a single spectrum. Samples of the background subtracted spectra are given in Fig. 11. For these cases the kinematically corrected yields, A_{Ne} and A_F were used to calculate R, and are given in Fig. 10. Within the uncertainty of about 20%, the ratio of yields is the same as the cross-section ratio. The vacancy-sharing ratio given by Meyerhof[36] fits the data well, whereas the cross-section ratio calculated in the BEA assuming the separated-atom binding energies does not. The same ratio can be calculated in the BEA assuming the united-atom (UA) correlated binding energies, but is much too small owing to the large binding energy of the UA K shell. If direct Coulomb ionization gives rise to UA $2p$ vacancies[38] which end up as F K-shell vacancies, then these vacancies are shared via a

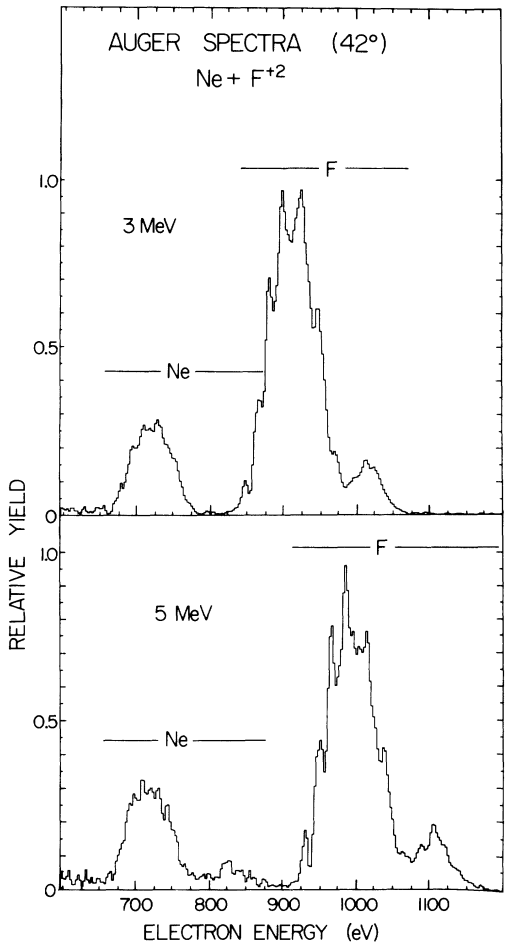

FIG. 11. Electron spectra for F^{+2} on Ne showing both the Ne K-shell electron lines and the F K-shell electron lines for 3- and 5-MeV F bombarding energy. A background of the exponential form, as discussed in the data-analysis section, has been subtracted from the spectra. The data have been divided by the electron energy to correct for the dispersion of the analyzer.

radial coupling as the nuclei recede from one another just as rotationally coupled vacancies would be.

V. CONCLUSION

The Ne-target K-shell Auger-electron production cross sections for H^+ bombardment from 0.5 to 10 MeV has been measured relative to the absolute measurement of Toburen[13] at 1.0 MeV. These measurements compare favorably with previous measurements as well as the predictions of calculations based on the BEA, PWBA, and Glauber approximations. These results confirm the accuracy of the measurement technique.

The Ne-target K-shell Auger-electron production cross section has been measured for N, O, F, and Cl bombardment of Ne for various incident charge states and, for F, over a large energy range. The measurement technique was the same as for H^+ bombardment. Within the experimental uncertainty the results for Cl bombardment agree with the results of Burch *et al.*[3] These heavy-ion-induced cross sections generally increase with increasing projectile charge state at fixed projectile energy. The most dramatic increases occur when the electron removed from the projectile is from the K shell. When a K-shell vacancy is present in the projectile, the cross section remains fairly constant as a function of projectile energy in the energy range studied. When no K-shell vacancies are present in the projectile, the cross section increases with increasing bombarding energy.

Below 15 MeV bombarding energy the F-projectile K-shell Auger-electron production cross section for collisions with Ne was also measured. When combined with the Ne-target cross-section measurements, the results have been compared favorably to MO calculations even though the collision velocities are, perhaps, too great for such a model to describe the collision in detail. The mechanism for production of the $2p\pi_x$ MO vacancies required for such a model is not clear. These $2p\pi_x$ vacancies must be produced in the collision since the $2p\pi$ orbital is correlated to the initially filled Ne $2p$ orbital. The fact that the cross section is similar for F^{+2} and F^{+3} bombardment indicates that the production of $2p\pi_x$ vacancies does not depend sensitively on the charge state of the projectile.

---

*Work supported in part by the U. S. Energy Research and Development Administration under Contract No. E(11-1)-2130.

†This work submitted in partial fulfillment of the requirements for the degree Doctor of Philosophy, Department of Physics, Kansas State University. Present address: Los Alamos Scientific Laboratory, Los Alamos, N. M. 87545.

‡Present address: Bell Laboratories, Murray Hill, N. J. 07974.

§Permanent address: Hahn-Meitner Institute, West Berlin, Germany.

[1]L. M. Winters, J. R. Macdonald, M. D. Brown, T. Chiao, L. D. Ellsworth, and E. W. Pettus, Phys. Rev. Lett. 31, 1344 (1973); and Phys. Rev. A 8, 1835 (1973).

[2]J. R. Mowat, I. A. Sellin, P. M. Griffin, D. J. Pegg, and R. S. Peterson, Phys. Rev. A 9, 644 (1974).

[3]D. Burch, N. Stolterfoht, D. Schneider, H. Wieman, and J. S. Risley, Phys. Rev. Lett. 32, 1151 (1974).

[4]R. L. Kauffman, C. W. Woods, K. A. Jamison, and P. Richard, Phys. Rev. A 11, 872 (1974).

[5]D. L. Matthews, B. M. Johnson, J. J. Mackey, L. E. Smith, W. Hodge, and C. F. Moore, Phys. Rev. A 10, 1177 (1974).

[6]D. Burch, W. B. Ingalls, J. S. Risley, and R. Heffner, Phys. Rev. Lett. 29, 1719 (1972).

[7]D. Schneider, D. Burch, and N. Stolterfoht, in *Abstracts of the Eighth International Conference on the Physics of Electronic and Atomic Collisions, Belgrade, 1973,* edited by B. C. Čobić and M. V. Kurepa (Institute of Physics, Belgrade, 1973), p. 729.

[8]D. L. Matthews, B. M. Johnson, J. J. Mackey, L. E. Smith, W. Hodge, and C. F. Moore, Phys. Rev. A 10, 451 (1974).

[9]C. F. Moore, J. J. Mackey, L. E. Smith, J. Bolger, B. M. Johnson, and D. L. Matthews, J. Phys. B 7, L302 (1974).

[10]C. P. Bhalla and M. A. Hein, Phys. Rev. Lett. 30, 39 (1973).

[11]C. P. Bhalla, N. O. Folland, and M. A. Hein, Phys. Rev. A 8, 649 (1973).

[12]J. S. Risley, Rev. Sci. Instrum. 43, 95 (1972), and references contained therein.

[13]L. H. Toburen, *Proceedings of the International Conference on Inner-Shell Ionization Phenomena and Future Applications, Atlanta, Georgia, 1972,* edited by R. W. Fink, S. T. Manson, J. M. Palms, and P. V. Rao, CONF-720404 (Natl. Tech. Information Service, U. S. Dept. of Commerce, Springfield, Va., 1972), p. 979; and private communication.

[14]The analyzer was designed by Erick Feldl with the assistance of Dr. C. L. Cocke and Dr. M. D. Brown, all of Kansas State University. The analyzer was constructed in the Precision Machine Shop at Kansas State University.

[15]H. Becker, E. Dietz, and U. Gerhardt, Rev. Sci. Instrum. 43, 1587 (1972).

[16]L. H. Toburen, Phys. Rev. A 3, 216 (1971).

[17]K. D. Sevier, *Low Energy Electron Spectroscopy* (Wiley-Interscience, New York, 1972).

[18]P. R. Bevington, *Data Reduction and Error Analysis for the Physical Sciences* (McGraw-Hill, New York, 1969).

[19]The 2-MeV cross section is measured relative to the 1-MeV cross section from Ref. 13.

[20]C. W. Woods, R. L. Kauffman, K. A. Jamison, C. L. Cocke, and P. Richard, J. Phys. B 7, L474 (1974).
[21]C. W. Woods, R. L. Kauffman, K. A. Jamison, N. Stolterfoht, and P. Richard, J. Phys. B 8, L61 (1975).
[22]A. K. Edwards and M. E. Rudd, Phys. Rev. 170, 140 (1968).
[23]M. O. Krause, F. A. Stevie, L. J. Lewis, T. A. Carlson, and W. E. Moddeman, Phys. Lett. 31A, 81 (1970).
[24]M. O. Krause, T. A. Carlson, and W. E. Moddeman, J. Phys. (Paris) 32, C4-139 (1971).
[25]N. Stolterfoht and D. Schneider, Phys. Rev. A 11, 721 (1975).
[26]J. H. McGuire and P. Richard, Phys. Rev. A 8, 1374 (1973).
[27]G. S. Kandelwal, B. H. Choi, and E. Merzbacher, At. Data 1, 103 (1969).
[28](a) J. E. Golden, Ph.D. dissertation (Kansas State University, Manhattan, Kan., 1975); and (b) J. E. Golden and J. H. McGuire, *Electronic and Atomic Collisions, Abstracts of the Papers of the Ninth International Conference on the Physics of Electronic and Atomic Collisions*, edited by J. S. Risley and R. Geballe (University of Washington Press, 1975), p. 507.
[29]J. E. Golden and J. H. McGuire (private communication).
[30]N. Stolterfoht, D. Schneider, D. Burch, B. Aagaard, E. Boving, and B. Fastrup, Phys. Rev. A 11, 1313 (1975).
[31]C. W. Woods, R. L. Kauffman, K. A. Jamison, N. Stolterfoht, and P. Richard, Phys. Rev. A 12, 1393 (1975).
[32]H. C. Brinkman and H. A. Kramer, Proc. Acad. Sci. (Amsterdam) 33, 973 (1930).
[33]U. Fano and W. Lichten, Phys. Rev. Lett. 14, 627 (1965).
[34]M. Barat and W. Lichten, Phys. Rev. A 6, 211 (1972).
[35]J. S. Briggs and J. Macek, J. Phys. B 5, 579 (1972).
[36]W. E. Meyerhof, Phys. Rev. Lett. 31, 1341 (1973).
[37]Yu. N. Demkov, Zh. Eksp. Teor. Fiz. 45, 195 (1963) [Sov. Phys.—JETP 18, 138 (1964)].
[38]C. Foster, T. Hoogkamer, P. Woerlee, and F. W. Saris, in Ref. 28(b), p. 511.
[39]K. Taulbjerg (private communication).